Available online at www.sciencedirect.com
ScienceDirect
Journal of Catalysis 248 (2007) 101–110
JOURNAL OF CATALYSIS
www.elsevier.com/locate/jcat

Production of hydrogen by catalytic reforming of dimethoxymethane over bifunctional catalysts

Yuchuan Fu, Jianyi Shen *

Laboratory of Mesoscopic Chemistry, School of Chemistry and Chemical Engineering, Nanjing University, Nanjing 210093, China

Received 8 December 2006; revised 11 March 2007; accepted 12 March 2007

Abstract

Reforming of hydrocarbons and oxygenated hydrocarbons is a potential way to supply H_2 for portable and household fuel cell applications. Of course, avoiding the use of toxic fuels is desirable. The extremely low toxicity of dimethoxymethane (DMM) may make it a preferred fuel for portable and household H_2 sources. We found that DMM can be effectively reformed to hydrogen on specially designed complex catalysts with bifunctional characters. The complex catalysts consisted of a traditional Cu–ZnO/γ-Al_2O_3 for the reforming of methanol and an acidic component for the hydrolysis of DMM. The acidity of the acidic component was found to be essential for the complex catalyst. A significant amount of dimethyl ether (DME) was produced when a strong solid acid such as H-ZSM-5 was used with the Cu–ZnO/γ-Al_2O_3 for the reforming of DMM. On the other hand, γ-Al_2O_3 exhibited low activity for the hydrolysis of DMM, resulting in the low efficiency of the complex catalyst. Tests showed that the acidic carbon nanofibers (H-CNF) seemed suitable as the acidic component in the complex catalysts. In fact, the complex catalysts Cu–ZnO/γ-Al_2O_3–H-CNF were found to exhibit excellent performance for the reforming of DMM. The rate of H_2 production from the reforming of DMM on the Cu–ZnO/γ-Al_2O_3–H-CNF could be as good as that from the reforming of methanol over the traditional Cu–ZnO/γ-Al_2O_3, whereas the reforming of DMM over the Cu–ZnO/γ-Al_2O_3 without an acidic component exhibited low activity and produced a significant amount of DME. Mechanistic studies showed that DME was produced from DMM on the Cu surface when no additional acidic component was present.

Keywords: Acidic carbon nanofibers; Copper catalyst; Dimethoxymethane; Hydrogen production; Steam reforming

1. Introduction

The production of H_2 through reforming of hydrocarbons and oxygenated organic compounds for fuel cells has been a common research focus in academia and industry for decades [1–3]. In particular, reforming of methanol and gasoline has received much attention. Methanol is easily reformed, and its use has been demonstrated by Daimler Chrysler in a prototype NECAR3 vehicle [4]. The disadvantage of using methanol as a fuel is that it is poisonous. This problem is even more serious when methanol is used in a microreformer for portable H_2 sources [5]. The advantage of using gasoline as a fuel for the production of H_2 is the existing infrastructure for the distribution of gasoline; however, the reforming of gasoline is much more difficult than that of methanol and involves more challenges [6,7]. The production of hydrogen from catalytic reforming of biomass-derived compounds [2,8] and dimethyl ether (DME) [9–11] also has been reported in recent years.

Generally, the production of H_2 for fuel cells from a carbon-containing compound involves reforming of the fuel, followed by the water–gas shift reaction (WGSR) and preferential oxidation (PROX) of CO in H_2 rich gas to reduce CO in the gas stream to an extent that can be tolerated by the anode of a proton-exchange membrane fuel cell (PEMFC). Because WGSR is exothermic, a low reaction temperature (e.g., 400–500 K) favors equilibrium and thus the low concentration of CO. However, the activity of the present WGSR catalysts is low at low temperatures [12,13], and recent efforts have been dedicated to exploring this issue [13–15]. The PROX process was developed to further reduce the concentration of CO in H_2-rich gas [5,16]. PROX requires the injection of O_2 into the stream of

* Corresponding author. Fax: +86 25 83317761.
E-mail address: jyshen@nju.edu.cn (J. Shen).

0021-9517/$ – see front matter
doi:10.1016/j.jcat.2007.03.013

H_2 to oxidize CO to CO_2. The O_2 injected is usually in excess of the stoichiometric amount for CO oxidation, and some fraction of H_2 is consumed [17,18]. Recent reports from Dumesic et al. [19,20] suggested a process for the use of reformate gas containing H_2 and CO for PEMFC. They used an intermediate (a reducible polyoxometalate compound [POM]) in the fuel cell; the POM was reduced by CO, and the reduced POM was readily oxidized on the anode to generate electricity. Through this process, the WGSR reaction is bypassed, and the CO can be used directly as an additional source of energy when the stream of H_2 is purified [20].

Dimethoxymethane (DMM), or methylal, has extremely low toxicity [21] and may be produced in a large scale [22]. Recently, it was reported that DMM can be produced by the direct oxidation of methanol [23,24], which will be more efficient if the process is industrialized. DMM is usually used as a solvent in pharmaceutical and perfume applications, as a methoxymethylation reagent in organic synthesis [25], and as an intermediate for the production of concentrated formaldehyde [26]. DMM is generally an environmentally benign chemical, being easily degraded in air with a lifetime of about 2 days, without the formation of organic peroxide intermediate and photochemical pollution [21].

Recently, we found that DMM can be effectively reformed to produce H_2 over Cu–ZnO/Al_2O_3-NbP complex catalysts [27]. The reforming of DMM by water can be considered to comprise reactions (1)–(3)—that is, the hydrolysis of DMM to form methanol and formaldehyde, which are then further reformed to produce H_2 and CO_2—although the actual pathways might be more complicated:

$$CH_3OCH_2OCH_3 + H_2O \rightarrow 2CH_3OH + CH_2O, \quad (1)$$

$$CH_3OH + H_2O \rightarrow 3H_2 + CO_2, \quad (2)$$

$$CH_2O + H_2O \rightarrow 2H_2 + CO_2. \quad (3)$$

The hydrolysis of DMM [Eq. (1)] requires an acidic catalyst, whereas the reforming of methanol and formaldehyde [Eqs. (2) and (3)] usually uses Cu–ZnO/γ-Al_2O_3 catalyst (designated CuZnAl below) [28,29]. Thus, an effective catalyst, comprising acidic and CuZnAl components, must be developed for the reforming of DMM.

Zeolites and γ-Al_2O_3 are two types of widely used solid acids. Typically, a zeolite has mainly Brønsted acid sites on its framework [30], whereas γ-Al_2O_3 exhibits mainly Lewis acidity [31]. The application of carbon nanofibers (CNFs) as catalyst supports has received extensive attention over the last 10 years [32–34]. It has been found that the catalytic behavior of nickel crystallites is altered dramatically when the metal is dispersed on CNFs compared with on activated carbon (AC) and γ-alumina [32]. Dong et al. [35] found that the addition of carbon nanotubes (CNTs) into the CuZnAl significantly enhances the catalytic activity for the synthesis of methanol. CNFs are usually oxidized by concentrated nitric acid or in a mixture of concentrated nitric and sulfuric acids before being used as catalyst supports. Such treatments result in the formation of large amounts of carboxylic and phenol groups, which are acidic [36]. Toebes et al. [37] studied the thermal stability of the acidic oxygen-containing groups in CNFs formed through the treatment with concentrated nitric acid and found that they were quite stable below 573 K. In the present work, we compared H-ZSM-5, γ-Al_2O_3, and acidic CNFs as acidic components for the hydrolysis of DMM and found that the surface acidity (nature and strength) of the acidic component is the essential factor in the effective reforming of DMM on complex catalysts.

2. Experimental

2.1. Preparation of catalysts

The bifunctional catalysts for the reforming of DMM were composed of a CuZnAl catalyst and an acidic component. The CuZnAl catalyst was prepared according to previous patents [38,39]. During preparation, precipitates were formed through three steps: (1) addition of an aqueous solution containing $Cu(NO_3)_2$ and $Zn(NO_3)_2$ into a solution of $NaHCO_3$ up to pH 7.0, to obtain a slurry (denoted as A); (2) addition of dilute solution of ammonia into the aqueous solution of $Al(NO_3)_3$ up to pH 7.0, to obtain a slurry of $Al(OH)_3$ (denoted as B); and (3) mixing of the slurries A and B to form a mixture that was stirred vigorously for 15 min and aged for 1 h. After washing, the precipitate was dried at 378 K for 12 h and calcined at 623 K for 3 h. The CuZnAl catalyst prepared contained 63% Cu, 21% Zn, and 16% Al in moles. The catalyst was pressed, crushed, and sieved to granules of 40–60 mesh for further use.

H-ZSM-5, γ-Al_2O_3, and acidic CNF (H-CNF) were used as the acidic components for the hydrolysis of DMM. The H-ZSM-5 (SiO_2/Al_2O_3 = 25, 450 $m^2\,g^{-1}$) and γ-Al_2O_3 (290 $m^2\,g^{-1}$) were commercial products and were calcined in air at 573 K for 3 h before the catalytic tests. The CNF was prepared by the decomposition of propylene on an unsupported Cu–Ni (4:6 by weight) catalyst following the procedure described by Shen et al. [40]. The H-CNF was obtained by treating the CNF in concentrated nitric acid (63 wt%). Specifically, 30 mL of concentrated nitric acid was added per 1 g CNF, and the mixture was refluxed for 30 min. Then the H-CNF was filtered, washed thoroughly with deionized water, and dried at 393 K for 12 h.

The complex catalysts containing H-ZSM-5 or γ-Al_2O_3 for the reforming of DMM were prepared by mixing with the CuZnAl. The resulting mixture was then ground, pressed, and sieved to granules of 40–60 mesh. The complex catalyst CuZnAl–H-CNF containing 12.5% H-CNF was prepared by adding the H-CNF into the solution of $Al(NO_3)_3$ before slurry B was formed for the preparation of the CuZnAl catalyst, whereas the complex catalysts containing 20 and 40% H-CNF were obtained by mixing in appropriate amounts of CuZnAl and H-CNF.

2.2. Characterization of catalysts

X-ray diffraction (XRD) patterns were collected in ambient atmosphere by an X-ray diffractometer (X'TRA, ARL Co., Switzerland) with Cu$K\alpha$ radiation (λ = 1.5418 Å). The 2θ

scans covered the range 10°–70°. The applied voltage and current were 40 kV and 40 mA, respectively. The reduced copper catalysts were passivated by flowing N_2 containing about 0.1% O_2 at room temperature for 12 h. Scherrer's equation was used for estimating the crystallite size of Cu in the catalysts according to the broadening of the XRD peak at $2\theta = 43.472°$.

Transmission electron microscopy (TEM) images were obtained using a JEM2100 instrument operated at 200 kV. Samples were prepared by suspending the catalysts in ethanol under ultrasonic vibration. Some drops of a suspension were brought onto a carbon film on a copper grid. The particle sizes were obtained by counting 50–100 particles in each sample. Scanning electron micrography (SEM) was done with a Hitachi S800 microscope at an accelerating voltage of 15 kV.

The surface areas of the catalysts were determined by N_2 adsorption at 77.3 K using the BET method. The active surface areas of copper in the catalysts were determined using the technique of adsorptive decomposition of N_2O at 363 K according to Chinchen et al. [41]. The surface areas of copper were calculated according to the amount of N_2 produced and the stoichiometric reaction $N_2O + 2Cu = Cu_2O + N_2$.

Temperature-programmed reduction (TPR) was performed using a quartz U-tube reactor loaded with about 50 mg of sample. A mixture of N_2 and H_2 (5.13% H_2 by volume) was used and the flow rate was maintained at 40 mL min^{-1}. The hydrogen consumption was monitored using a thermal conductivity detector (TCD). The temperature was raised from 303 to 1173 K at a programmed rate of 5 K min^{-1}.

Microcalorimetric measurements of ammonia adsorption were performed to determine the surface acidity of the samples at 423 K. A Setaram C-80 calorimeter was connected to a volumetric system equipped with a Baratron capacitance manometer for the pressure measurement and gas handling. Before the microcalorimetric adsorption of ammonia, HZSM-5 and γ-Al_2O_3 were activated at 673 K in 500 Torr O_2, followed by evacuation at the same temperature for 1 h, whereas the CNF samples were directly outgassed at 533 K for 1 h. After thermal equilibrium was reached for a sample in vacuum at 423 K, microcalorimetric data were collected with probe molecules of NH_3 dosed sequentially. Elemental analysis was performed using an inductively coupled plasma method.

2.3. Tests of catalytic activity

The catalytic reactions for the hydrolysis and reforming of DMM were performed in a fixed-bed microreactor. The DMM and H_2O were introduced to the reaction zone by bubbling N_2 (99.999%) through a glass saturator filled with DMM (Aldrich, 99%) maintained at 273 K and a glass saturator filled with H_2O maintained at 333 K, respectively. The feed composition was maintained at N_2:H_2O:DMM = 24:5:1 (v/v). The catalysts containing copper were prereduced at 533 K (raised from room temperature at a rate of 1 K min^{-1}) for 3 h in 12% H_2/N_2 at a flow rate of 50 mL min^{-1}. The products were analyzed by an online gas chromatograph equipped with an FID and a TCD. The FID was connected to a Porapak N column for the separation of methanol, DMM and other organic compounds, and the TCD was connected to a TDX-01 column for the analysis of methane, CO_x, and N_2. The amount of H_2 produced was usually calculated according to the conversion of DMM and the composition of other products and was checked using another gas chromatograph with a TDX-01 column. (This gas chromatograph also can be used for the analysis of formaldehyde when switched to a Porapak-N column when necessary.) The reforming of methanol was also performed for comparison.

The selectivity to H_2 for the reforming of DMM was defined as the total mol of H_2 actually produced divided by the mol of H_2 theoretically produced according to the reaction $CH_3OCH_2OCH_3 + 4H_2O = 3CO_2 + 8H_2$ [27]. The selectivity to a carbonaceous product is defined as the amount of carbon in this product divided by the total amount of carbon in converted DMM. The byproducts found were CH_4, CH_3OH, and DME.

3. Results and discussion

3.1. Characterization of catalysts

Fig. 1 shows the SEM images of the as-prepared (CNF) and nitric acid-treated (H-CNF) CNFs. The particles in these samples had an average diameter of about 300 nm and surface areas of 175 m^2 g^{-1} for CNF and 169 m^2 g^{-1} for H-CNF. Treatment with nitric acid did not seem to cause any significant changes in morphology and surface area, but it did rupture some fibers. In addition, the XRD data (not shown here) revealed that the graphite phase of the CNF was not changed and no metal impurities (Cu or Ni) were detected in the CNF after the treatment with nitric acid.

Fig. 2 shows the XRD patterns of the CuZnAl and CuZnAl–12.5% H-CNF catalysts calcined at 623 K. The phases detected in the CuZnAl were mainly CuO and some $ZnCO_3$ and $Cu_6Al_2(OH)_{16}CO_3$. Incorporation of H-CNF seemed to retard the decomposition of precursors of CuO, because substantial amounts of $Cu_2(OH)_2CO_3$ was detected in the CuZnAl–12.5% H-CNF sample. This might be due to the decomposition of carboxylic groups on the surface of H-CNF, which released CO_2 and inhibited the decomposition of $Cu_2(OH)_2CO_3$. The average particle sizes of CuO in the CuZnAl and CuZnAl–12.5% H-CNF catalysts were estimated as 11 and 10 nm, respectively, according to Scherrer's method. The XRD patterns of the catalysts after reduction are shown in Fig. 3. Both samples exhibited essentially the same features of metallic copper and ZnO after reduction. In addition, the average sizes of metallic copper particles as determined by Scherrer's method were almost the same (13 nm) for the two catalysts.

The number of surface copper atoms was found to be 557 μmol g_{cat}^{-1} for CuZnAl and 483 μmol g_{cat}^{-1} for CuZnAl–12.5% H-CNF by the adsorptive decomposition of N_2O. The dispersion of metallic Cu (7.8 and 7.9%), as well as the crystallite size of the copper particles (13.4 and 13.2 nm), were found to be almost the same for the two samples.

Fig. 4 compares the TEM images of the pure CuZnAl catalyst with that of the complex CuZnAl–12.5% H-CNF catalyst before and after reduction. The particles seen in the images of the nonreduced catalysts are irregular, with an average size of

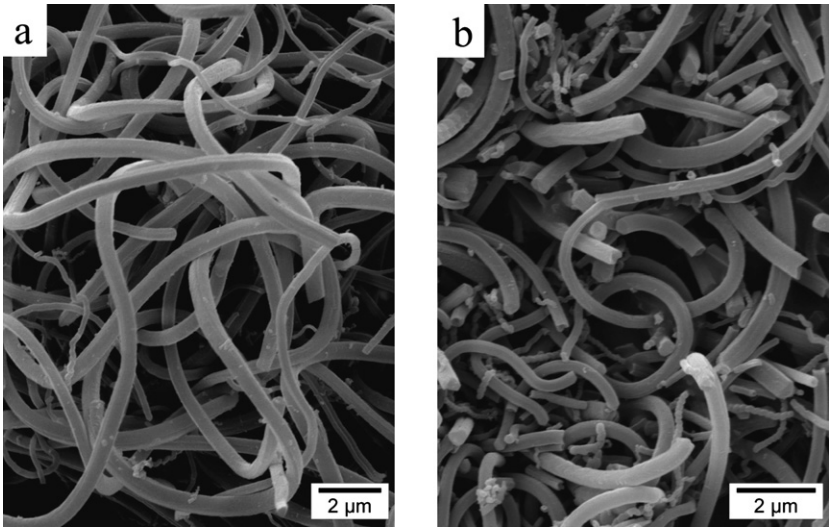

Fig. 1. SEM images of carbon nanofibers: (a) as-prepared and (b) refluxed in 63% HNO_3 for 30 min.

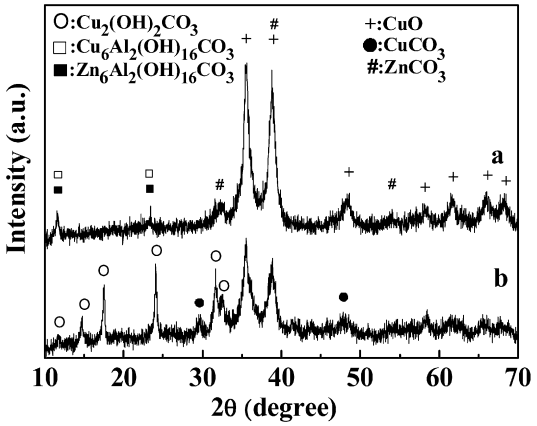

Fig. 2. X-ray diffraction patterns of (a) CuZnAl and (b) CuZnAl–12.5% H-CNF catalysts after calcination at 623 K.

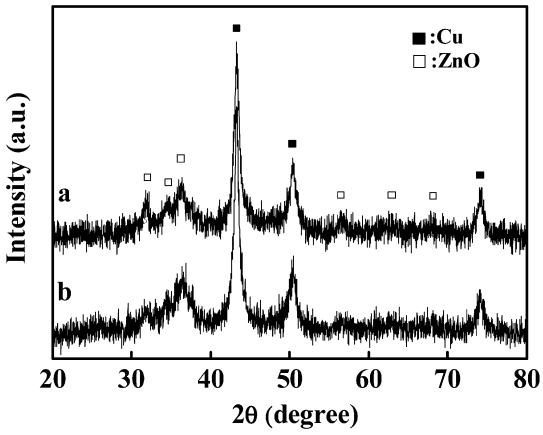

Fig. 3. X-ray diffraction patterns of (a) CuZnAl and (b) CuZnAl–12.5% H-CNF catalysts after reduction at 533 K in 12% H_2/N_2 for 3 h and passivation at room temperature in about 0.1% O_2/N_2 for 12 h.

about 15 nm, although the phases of the particles might be different for different catalysts. The particles in the CuZnAl before reduction (Fig. 4a) may be mainly CuO with some $ZnCO_3$ and $Cu_6Al_2(OH)_{16}CO_3$, as revealed by XRD. The particles attached to the surface of carbon fiber in Fig. 4b might be the mixture of CuO and $Cu_2(OH)_2CO_3$ before reduction (see Fig. 2b). Figs. 4a′ and 4b′ present TEM images of the two catalysts after reduction. The spherical particles seen in Fig. 4a′ might be the 10- to 20-nm particles of metallic copper, consistent with those determined according to the XRD peak width and Scherrer's equation, as well as the N_2O adsorption. A similar result was found for the CuZnAl–12.5% H-CNF catalyst after reduction, with 10- to 20-nm metallic copper particles attached to the surface of carbon fiber clearly visible (Fig. 4b′).

The results of microcalorimetric adsorption of ammonia are presented in Fig. 5. The coverage of ammonia is usually defined as the amount of ammonia adsorbed with the differential heat $>40\ kJ\,mol^{-1}$. The as-prepared CNF was nonacidic, because the associated heat of adsorption of NH_3 was $<10\ kJ\,mol^{-1}$. Treatment with nitric acid greatly increased its surface acidity. The initial heat and NH_3 coverage for H-CNF were found to be about $150\ kJ\,mol^{-1}$ and $330\ \mu mol\,g^{-1}$, respectively. This result is consistent with that reported by Toebes et al. [37] for the nitric acid-treated CNF [37]. The number of acid sites on the surface of our H-CNF as titrated by NH_3 was $1.2\ nm^{-2}$. Although the surface acidity of the H-CNF was decreased on reduction at 533 K in 12% H_2/N_2 (a condition used for the reduction of CuZnAl), it still had substantial surface acidity with an initial heat of about $125\ kJ\,mol^{-1}$ and a coverage of $260\ \mu mol\,g^{-1}$ for the adsorption of ammonia. The surface acidity of H-ZSM-5 was strong with the initial heat of about $180\ kJ\,mol^{-1}$ and coverage of about $700\ \mu mol\,g^{-1}$ for the adsorption of NH_3. The initial heat and coverage for ammonia adsorption on the γ-Al_2O_3 were about $220\ kJ\,mol^{-1}$ and $400\ \mu mol\,g^{-1}$, respectively. The surface acidity of the γ-Al_2O_3 was weaker than that of H-ZSM-5, but stronger than that of H-CNF in terms of the microcalorimetric adsorption of ammonia.

The results of TPR for the CuZnAl and CuZnAl–12.5% H-CNF catalysts are compared in Fig. 6. The two samples exhibited similar TPR profiles with three peaks each. These peaks may indicate the reduction of different copper precursors to metallic copper in the catalysts. The addition of H-CNF

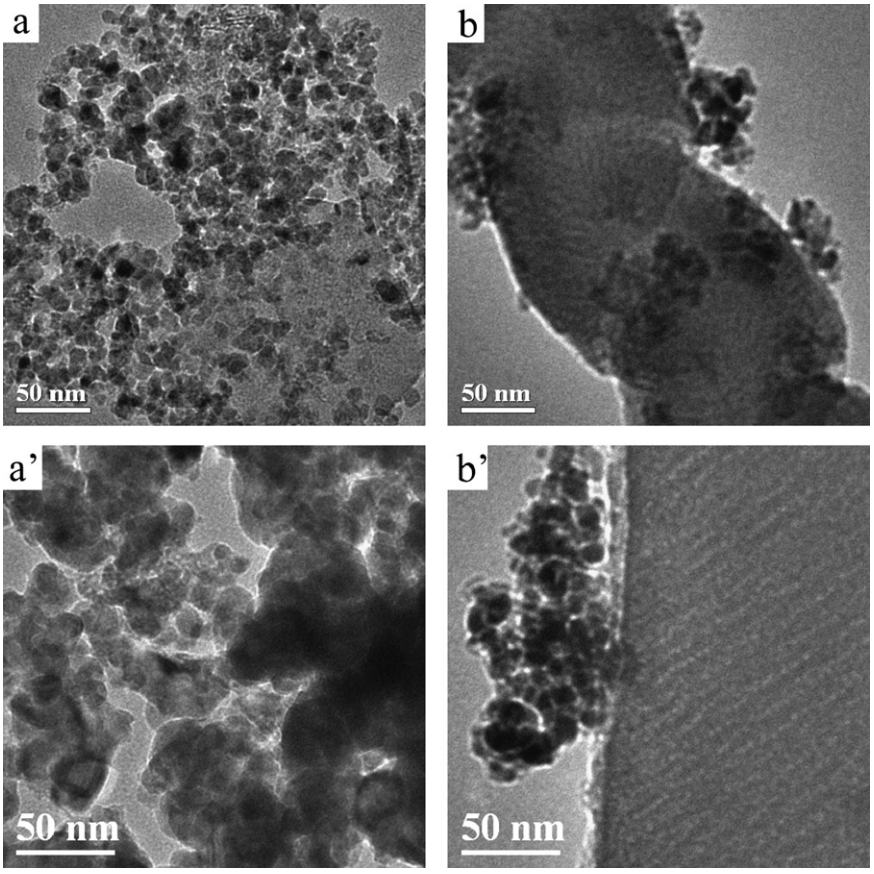

Fig. 4. TEM images for CuZnAl before (a) and after (a′) the reduction, as well as for CuZnAl–12.5% H-CNF before (b) and after (b′) the reduction. The reduction was performed at 533 K in 12% H_2/N_2 for 3 h, followed by passivation at room temperature in about 0.1% O_2/N_2 for 12 h.

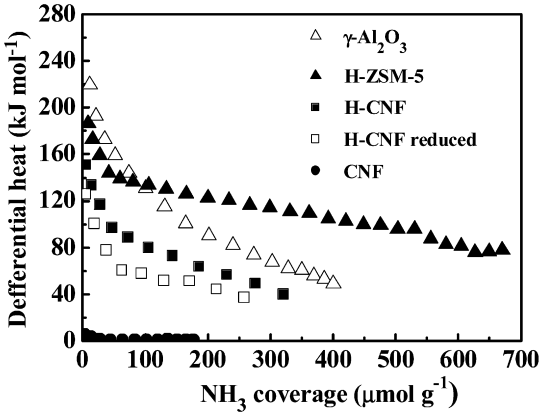

Fig. 5. Differential heat versus coverage for NH_3 adsorption at 423 K over H-ZSM-5, γ-Al_2O_3, CNF, H-CNF, and H-CNF reduced at 533 K in 12% H_2/N_2 for 3 h.

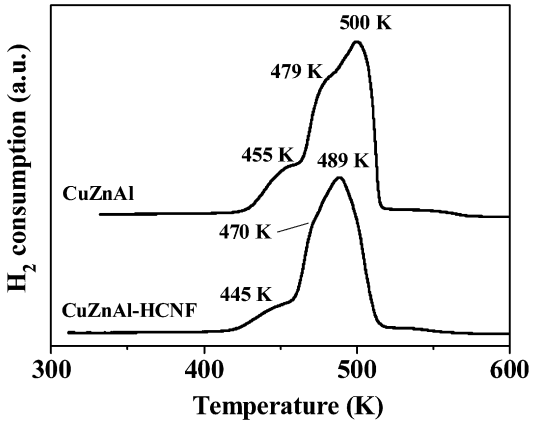

Fig. 6. Temperature-programmed reduction profiles of CuZnAl and CuZnAl–12.5% H-CNF catalysts.

seemed to promote the reduction of copper species, because each TPR peak shifted to the lower temperature for CuZnAl–12.5% H-CNF compared with CuZnAl. This result is consistent with the findings of Dong et al. [35], who reported that the addition of CNT lowered the reduction temperatures of the copper-based catalysts for methanol synthesis.

Table 1 summarizes some physical properties of the CuZnAl and CuZnAl–12.5% H-CNF catalysts. The data in Table 1 show that the main physical properties of the two catalysts in terms of surface area of the catalysts, active surface area of copper, and dispersion and particle size of copper were essentially the same. Thus, the addition of H-CNF did not seem to affect the main physical properties of the CuZnAl catalyst.

3.2. Hydrolysis of DMM

Table 2 presents the results for the hydrolysis of DMM over H-ZSM-5, γ-Al_2O_3, and H-CNF. The conversion of DMM on

Table 1
Physical properties of the CuZnAl and CuZnAl–12.5% H-CNF catalysts

Catalyst	S_{BET} ($m^2\ g^{-1}$)	wt% of Cu	Copper on the surface[a]		Dispersion of Cu (%)	d_{copper} (nm)[b]	d_{copper} (nm)[c]
			($m^2\ g_{cat}^{-1}$)	($\mu mol\ g_{cat}^{-1}$)			
CuZnAl	99	45.2	22.8	557	7.8	13.4	13.1
CuZnAl–12.5% H-CNF	101	38.9	19.8	483	7.9	13.2	13.3

[a] Determined by using the technique of adsorptive decomposition of N_2O.
[b] Particle size of metallic copper as calculated according to the dispersion of copper.
[c] Particle size of metallic copper as calculated according to the Sherrer's equation.

Table 2
Hydrolysis of DMM over H-ZSM-5, γ-Al_2O_3 and H-CNF[a]

Catalyst	Temp. (K)	GHSV ($ml\ g_{cat}^{-1}\ h^{-1}$)	DMM conv. (%)	Selectivity (%)[b]	
				Methanol	DME
H-ZSM-5	473	2.0×10^5	98.1	60.6	39.4
	493	2.0×10^5	99	45.9	54.1
γ-Al_2O_3	473	2.3×10^4	2.9	99.3	0.7
	493	2.3×10^4	8.3	96.2	3.8
	513	2.3×10^4	15.6	97.7	2.3
H-CNF[c]	473	9.0×10^4	93.4	98.4	1.6
	493	9.0×10^4	98.2	98.3	1.7
	513	9.0×10^4	98.3	98.9	1.1

[a] Feed composition: $N_2/H_2O/DMM = 24/5/1$ (v/v).
[b] The selectivity to methanol and DME was normalized, and other products such as formaldehyde, methyl formate and trace of methane were not included.
[c] Prior to the hydrolysis test, the H-CNF was reduced at 533 K in 12% H_2/N_2 for 3 h, which was the same condition for the reduction of CuZnAl–H-CNF for the reforming of DMM.

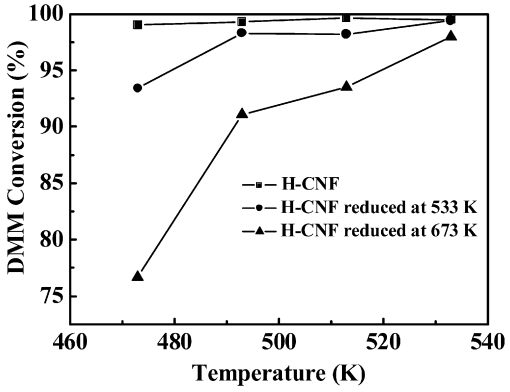

Fig. 7. Effect of reduction of H-CNF at different temperatures in 12% H_2/N_2 on the hydrolysis of DMM. Reaction conditions: $N_2/H_2O/DMM = 24/5/1$ (v/v) and GHSV $= 9.0 \times 10^4\ ml\ g^{-1}\ h^{-1}$.

H-ZSM-5 was high (>98%) with a substantial amount of DME as the hydrolysis product at 473 and 493 K. Apparently, the methanol produced from the hydrolysis of DMM was further converted to DME over this strong solid acid. Thus, H-ZSM-5 does not seem to be suitable as an acidic component for the reforming of DMM. In contrast, the γ-Al_2O_3 exhibited low conversion of DMM up to 513 K (15.6%), although the selectivity to methanol was high for the hydrolysis of DMM. Thus, a high fraction of γ-Al_2O_3 would be required for the complex catalyst, which would lower the efficiency of DMM reforming. Data in Table 2 show that the H-CNF exhibited high activity with high selectivity to methanol for the hydrolysis of DMM. For example, both the conversion of DMM and selectivity to methanol were >98% on the H-CNF at 493 K with space velocity four times greater than that for the hydrolysis of DMM on γ-Al_2O_3. These results clearly indicate that the choice of solid acid with proper surface acidity might be the essential factor in determining the catalytic behavior of the complex catalysts for the reforming of DMM to produce H_2. It should be mentioned that before the hydrolysis test, the H-CNF was reduced at 533 K in 12% H_2/N_2 for 3 h, the same condition for the reduction of CuZnAl and CuZnAl–H-CNF. The stability of surface acidity of H-CNF resistant to the reduction by H_2 is important, because the reforming of DMM is performed under the reducing atmosphere.

The effect of reduction of H-CNF by H_2 on the hydrolysis of DMM was further investigated; the results are shown in Fig. 7. The activity of H-CNF was high for the hydrolysis of DMM; the conversion of DMM was 100% over H-CNF at 473 K. In fact, microcalorimetric adsorption of ammonia showed that the H-CNF exhibited fairly strong surface acidity with the initial heat of 150 $kJ\ mol^{-1}$ and coverage of 330 $\mu mol\ g^{-1}$ for the adsorption of NH_3. The reduction in 12% H_2/N_2 at 533 K decreased the surface acidity (Fig. 5) and thus decreased the activity for the hydrolysis of DMM. The surface acidity of CNF would be further decreased if reduction were done at higher temperatures. Accordingly, the activity of H-CNF for the hydrolysis of DMM decreased with increasing temperature of reduction. The data in Fig. 7 show that when the hydrolysis of DMM was carried out at 473 K, the conversion of DMM over the H-CNF was about 93% when reduced at 533 K and 76% when reduced at 673 K. These results indicate that the acidic functional groups on the surface of H-CNF might be responsible for the hydrolysis of DMM. Although the conversion of DMM was lower on the H-CNF reduced at 673 K compared with the nonreduced H-CNF for the hydrolysis of DMM at 473 K, the activity of the reduced H-CNF was still much higher than that of γ-Al_2O_3. For example, the rate of DMM conversion over the H-CNF reduced at 673 K was much higher than that over the γ-Al_2O_3 for the hydrolysis of DMM (about 100 times higher when reduced at 473 K and 20 times higher when reduced at 513 K). The conversion of DMM was about 96% on the H-CNF reduced at 673 K for the hydrolysis of DMM at 533 K. Stable surface acidity of H-CNF is the primary requirement for a stable complex catalyst CuZnAl–H-CNF for the reforming of DMM.

The microcalorimetric results show that the surface acidity of γ-Al_2O_3 was stronger than that of H-CNF in terms of the initial heat and uptake for the adsorption of NH_3. However, the activity of γ-Al_2O_3 was much lower than that of H-CNF sam-

Table 3
Reforming of DMM over the CuZnAl and complex catalysts[a]

Catalyst[b]	DMM			Selectivity to carbonaceous products (%)				
	Temp. (K)	Conv. (%)	H_2 sel. (%)	CO	CO_2	CH_3OH	DME	CH_4
CuZnAl	493	2.8	87.1	n.d.[c]	88.6	2.9	8.2	0.3
	513	6.9	84.5	n.d.[c]	86.5	1.3	11.6	0.6
	533	14.8	81.2	n.d.[c]	83.6	0.8	14.7	0.8
	553	30.2	77.9	n.d.[c]	80.8	0.5	17.4	1.3
CuZnAl–H-ZSM-5	493	100	62.0	0.2	65.9	1.2	32.4	0.0
	513	100	78.0	1.2	80.9	1.0	17.2	0.9
CuZnAl–γ-Al_2O_3	473	5.6	79.9	n.d.[c]	82.2	7.7	9.8	0.3
	493	30.2	94.0	n.d.[c]	94.7	1.5	3.7	0.1
	513	79.5	96.2	1.0	96.0	0.9	2.0	0.1
	533	99.9	95.3	6.5	91.5	0.0	1.9	0.1
	553	100	93.7	10.3	87.6	0.0	2.0	0.1
CuZnAl–H-CNF	473	37.8	93.8	n.d.[c]	94.5	3.2	2.2	0.1
	493	99.6	98.3	0.3	98.4	0.4	0.9	0.1
	513	100	97.5	4.3	94.9	0.0	0.8	0.0
	533	100	96.5	6.9	92.3	0.0	0.7	0.0

[a] Conditions for DMM reforming: $N_2/H_2O/DMM = 24/5/1$ (v/v) and GHSV $= 4.55 \times 10^3$ ml g_{cat}^{-1} h^{-1}.
[b] The content of HZSM-5, γ-Al_2O_3, and H-CNF in the complex catalysts was 25, 33, and 12.5%, respectively.
[c] Not detectable.

ples for the hydrolysis of DMM. This might be due to the fact that the acid sites on γ-Al_2O_3 are mainly Lewis type [31], and the strong Lewis acid sites might be converted into weak Brønsted sites when H_2O was adsorbed during the reaction of DMM hydrolysis [42,43]. On the other hand, this phenomenon might reflect the nature of surface acidity. The acid sites on H-CNF are known to be the surface carboxylic and phenol groups [36], which are Brønsted type in nature. In addition, niobium phosphate exhibited mainly Brønsted acidity and high activity for the hydrolysis of DMM [27]. Thus, the solid acids with fairly strong Brønsted acidity seemed to be a suitable acidic component for the reforming of DMM to produce H_2. In contrast, strong Brønsted solid acids, such as H-ZSM-5, and Lewis solid acids, such as γ-Al_2O_3, did not function properly in this role.

3.3. Reforming of DMM

Table 3 presents the results for the reforming of DMM over CuZnAl as well as the complex catalysts CuZnAl–HZSM-5, CuZnAl–γ-Al_2O_3, and CuZnAl–H-CNF. For comparison, the complex catalysts comprised 25% HZSM-5, 33% γ-Al_2O_3, and 12.5% H-CNF. The CuZnAl catalyst exhibited low activity for the reforming of DMM and produced a significant amount of DME as a byproduct, probably due to the lack of acidic sites in the catalyst (we address this issue further in Section 3.4).

The conversion of DMM was greatly enhanced on the addition of any of the acidic components. It seems that the catalytic behavior of the complex catalysts for the reforming of DMM is closely related to the catalytic behavior of the corresponding acid components for the hydrolysis of DMM. The activity of CuZnAl–H-ZSM-5 for the reforming of DMM was high, with 100% conversion of DMM at 473 K, but the selectivity to H_2 was low due to the formation of substantial amount of DME. In addition, some light hydrocarbons were also produced during the reforming of DMM over the CuZnAl–H-ZSM-5 at temperatures above 513 K.

The complex catalyst CuZnAl–γ-Al_2O_3 exhibited much higher activity than the pure CuZnAl for the reforming of DMM. In addition, the selectivity to H_2 was high for the reforming of DMM over the CuZnAl–γ-Al_2O_3. However, the conversion of DMM was low at the temperatures below 513 K, due to the low activity of γ-Al_2O_3 for the hydrolysis of DMM. The conversion of DMM increased with increasing reaction temperature and achieved 100% at 533 K. It is interesting to note that the selectivity to H_2 over the CuZnAl–γ-Al_2O_3 passed through a maximum with the increase of reaction temperature from 473 to 553 K. At 473 K, γ-Al_2O_3 exhibited low activity for the hydrolysis of DMM; thus, some of the DMM was directly converted to DME on the surface of CuZnAl. The activity of γ-Al_2O_3 for the hydrolysis of DMM increased with increasing reaction temperature, leading to increased selectivity to H_2 for the reforming of DMM on complex catalyst CuZnAl–γ-Al_2O_3. However, the selectivity to H_2 would decrease with further increases in the reaction temperature, due to the equilibrium limitation of the WGSR.

The CuZnAl–12.5% H-CNF catalyst exhibited high activity and selectivity to H_2 for the reforming of DMM even at relatively low reaction temperatures. For example, the conversion of DMM over the CuZnAl–12.5% H-CNF was nearly 100% at 493 K, 40 K lower than the reaction temperature for the same conversion of DMM over the CuZnAl–γ-Al_2O_3. Apparently, the high efficiency of the CuZnAl–12.5% H-CNF for the reforming of DMM results from the high activity and selectivity of the H-CNF for the hydrolysis of DMM to methanol and formaldehyde. High temperature would cause the sintering of copper crystallite and accelerate the deactivation of CuZnAl catalyst [44]; thus, the low reaction temperature enhances the durability of the complex catalysts. Moreover, a low reaction temperature favors a low concentration of CO in the refor-

Table 4
Comparison of the rate of hydrogen production from the reforming of DMM and methanol at 513 K

Catalyst	Fuel	GHSV ($ml\ g_{cat}^{-1}\ h^{-1}$)	Conv. (%)	Rate of H_2 production		Selectivity (%)				
				($ml\ g_{cat}^{-1}\ h^{-1}$)	($H_2\ Cu^{-1}\ s^{-1}$)[c]	H_2	CO	CO_2	CH_3OH	DME
CuZnAl	CH_3OH[a]	2.6×10^4	94.2	5230	0.12	99.8	0.7	99.3	–	0.0
CuZnAl–12.5% H-CNF	CH_3OH[a]	2.6×10^4	91.6	5090	0.13	99.8	0.6	99.4	–	0.0
CuZnAl–12.5% H-CNF	DMM[b]	2.1×10^4	45.9	2500	0.06	97.4	n.d.[d]	97.7	1.1	1.2
CuZnAl–20% H-CNF	DMM[b]	2.1×10^4	77.3	4130	0.11	95.6	n.d.[d]	96.1	3.6	0.3
CuZnAl–40% H-CNF	DMM[b]	2.1×10^4	99.7	5200	0.19	93.0	0.6	93.3	6.1	0.0

[a] Feed conditions for methanol reforming: $N_2/H_2O/CH_3OH = 11.8/1.25/1$ (v/v).
[b] Feed conditions for DMM reforming: $N_2/H_2O/DMM = 24/5/1$ (v/v).
[c] Molecules of H_2 per atom of surface Cu per second.
[d] Not detectable.

mate gas, because it is determined mainly by the equilibrium of WGSR.

Table 4 shows the results of reforming of methanol and DMM over the CuZnAl and CuZnAl–H-CNF with varying H-CNF content at 513 K. The reforming of methanol over the CuZnAl and CuZnAl–12.5% H-CNF was essentially the same in terms of conversion of methanol, rate of hydrogen production, and selectivity to H_2, implying that the addition of H-CNF did not affect the catalytic behavior of CuZnAl for the reforming of methanol.

The data in Table 4 also show the effect of the amount of H-CNF in CuZnAl–H-CNF on the reforming of DMM. The conversion of DMM was much lower than that of methanol over CuZnAl–12.5% H-CNF at 513 K with similar space velocity. The conversion of DMM increased with an increasing amount of H-CNF in CuZnAl–H-CNF for the reforming of DMM. The conversion of DMM was found to be 77.3% for the complex catalyst containing 20% H-CNF and 99.7% for that containing 40% H-CNF. The rate of H_2 production was also increased accordingly, reaching about 5200 $ml\ g_{cat}^{-1}\ h^{-1}$ for the reforming of DMM over CuZnAl–40% H-CNF at 513 K, almost the same as that from the reforming of methanol over CuZnAl at the same temperature with similar space velocity (5230 $ml\ g_{cat}^{-1}\ h^{-1}$), with conversions of methanol and DMM reaching 94.2 and 99.7%, respectively.

This result demonstrates that the reforming of DMM over the complex CuZnAl–H-CNF catalysts could be as effective as that of methanol over CuZnAl. In addition, when the activity is calculated based on the number of copper sites on the surface, the rate of H_2 production was much higher for the reforming of DMM on CuZnAl–40% H-CNF (0.19 molecules of H_2 per atom of surface Cu per second) than that of methanol on CuZnAl (0.12 molecules of H_2 per atom of surface Cu per second).

It is generally known that the reforming of methanol involves the dissociative adsorption of methanol to form the surface methoxy groups [Eq. (4)] [29,45,46], with the abstraction of an additional H from the methoxy group to form adsorbed formaldehyde [Eq. (5)] as the rate-determining step [29,47]. This implies that the following steps that could be taken as the reforming of formaldehyde were relatively fast.

$$CH_3OH + 2^* \rightarrow CH_3O^* + H^* \quad (4)$$

and

$$CH_3O^* + ^* \rightarrow CH_2O^* + H^*. \quad (5)$$

Because the hydrolysis of 1 mol of DMM produced 2 mol of methanol and 1 mol of formaldehyde (with formaldehyde reformed much faster than methanol), the rate of H_2 production from the reforming of DMM over CuZnAl–H-CNF must be 33% greater than that from the reforming of methanol over CuZnAl as long as the hydrolysis of DMM is sufficiently rapid on acid sites. Thus, if a better acidic component than H-CNF could be developed and used with CuZnAl for the reforming of DMM, then the mass ratio of CuZnAl in the complex catalyst could be higher, and a higher rate of H_2 production might be achieved. In this case, H_2 production from the reforming of DMM on the complex catalyst might be more effective than that from the reforming of methanol on CuZnAl.

The concentration of CO in the reformate gas produced from the reforming of methanol is determined mainly by the equilibrium of the WGSR [27]. Similarly, the CO concentration in the reformate gas from the reforming of DMM is close to the equilibrium value of WGSR when the conversion of DMM is close to 100%, as calculated according to the data in Table 3 for the CuZnAl–H-CNF at temperatures above 513 K.

3.4. Mechanistic aspect of DME formation on CuZnAl

The data in Table 3 show that the reforming of DMM over CuZnAl exhibited low activity and produced a significant amount of DME. One apparent reason for the low activity in the CuZnAl catalyst was a lack of acidity for the hydrolysis of DMM. Thus, understanding why DMM was converted into DME over CuZnAl is of importance. Because the reforming of methanol over CuZnAl produces mainly H_2 with little DME, there must be a pathway for the formation of DME from DMM over CuZnAl. The degradation of DMM over the copper surface might involve the following pathways:

$$CH_3OCH_2OCH_3 + MO + M \rightarrow MOCH_3 + CH_3OCH_2OM, \quad (6)$$

$$MOCH_2OCH_3 + MO + M \rightarrow MOCH_3 + MOCH_2OM, \quad (7)$$

$$MOCH_2OCH_3 + MOCH_3 \rightarrow MOCH_2OM + CH_3OCH_3, \quad (8)$$

$$MOCH_2OM \rightarrow 2M + H_2 + CO_2, \quad (9)$$

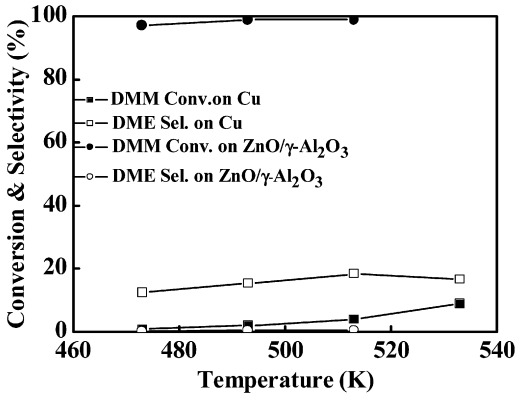

Fig. 8. Selectivity to DME over unsupported Cu and ZnO/γ-Al_2O_3 for the reforming of DMM. Reaction conditions: $N_2/H_2O/DMM = 24/5/1$ (v/v) and GHSV $= 4.55 \times 10^3$ ml g_{cat}^{-1} h^{-1}.

$$2MOCH_3 \rightarrow MO + M + CH_3OCH_3, \quad (10)$$

$$MO + M + H_2O \rightarrow 2MOH, \quad (11)$$

and

$$MOCH_3 + MOH \rightarrow MO + M + CH_3OH, \quad (12)$$

where M denotes the Cu surface. It has been established that adsorbed oxygen species exist on the surface of copper when H_2O is present in the reaction system [46,48]. Both DMM and methanol could be dissociatively adsorbed on Cu to produce surface methoxy groups. Although the surface methoxy groups can be combined to form DME as Eq. (10), this step might be a minor reaction for the formation of DME, because surface methoxy groups might be readily converted into H_2 and CO_2 on CuZnAl [29]. In fact, the reforming of methanol produced little DME despite the fact that the adsorption of methanol produced large amounts of surface methoxy groups [29]. Therefore, there must be pathways from DMM to DME over the Cu surface that are not via two methoxy groups. Equation (8) might be such a step in the formation of DME from DMM on Cu.

To confirm that DME was produced from DMM on Cu rather than on ZnO/γ-Al_2O_3, we prepared an unsupported Cu sample (23 m^2 g^{-1} before reduction) and a ZnO/γ-Al_2O_3 sample (142 m^2 g^{-1}) for the reforming of DMM. Fig. 8 shows that little DME was formed over the ZnO/γ-Al_2O_3, whereas the selectivity to DME was as high as 18% over the unsupported Cu at 513 K. These results clearly demonstrate the existence of a pathway for the formation of DME from DMM on the Cu surface.

4. Conclusion

This work has demonstrated that DMM can be effectively reformed to hydrogen on specially designed complex catalysts with bifunctional character, comprising an acidic component and a traditional CuZnAl catalyst. The basic chemistry for the reforming of DMM involves the hydrolysis of DMM on acidic sites to form methanol and formaldehyde, which are then reformed to produce H_2 and CO_2. The rate of H_2 production through the reforming of DMM over the complex catalysts could be as good as that of the traditional method of reforming methanol on the CuZnAl catalyst. The traditional CuZnAl catalyst alone exhibited low activity for the reforming of DMM and produced a significant amount of DME on the copper surface. The addition of an acidic component with proper nature and strength is essential for the reforming of DMM. H-ZSM-5 is a strong solid acid that is not suitable for the hydrolysis of DMM due to the formation of a significant amount of dimethyl ether, and the Lewis solid acid γ-Al_2O_3 is not sufficiently active for the hydrolysis of DMM.

Our findings demonstrate that H-CNF may be a good acidic component. The H-CNF has stable Brønsted acidity that effectively catalyzes the hydrolysis of DMM. Accordingly, the addition of H-CNF into CuZnAl formed complex catalysts CuZnAl–H-CNF, which catalyzed the reforming of DMM with high activity and selectivity to H_2. Because DMM is a nonpoisonous and environmentally benign compound, it may be a more appropriate fuel for portable and household H_2 sources for fuel cells.

Acknowledgments

This work was supported by the Ministry of Science and Technology of China (Grants 2004DFB02900 and 2005CB22-1403) and the National Science Foundation of China (Grant 20373023).

References

[1] A. Qi, S. Wang, G. Fu, C. Ni, D. Wu, Appl. Catal. A 281 (2005) 233.
[2] R.D. Cortright, R.R. Davda, J.A. Dumesic, Nature 418 (2002) 964.
[3] J.C. Amphlett, R.F. Mann, B.A. Peppley, P.R. Roberge, A. Rodrigues, J.P. Salvador, J. Power Sources 71 (1998) 179.
[4] F. Panik, J. Power Sources 71 (1998) 36.
[5] C. Song, Catal. Today 77 (2002) 17.
[6] D.J. Moon, K. Sreekumar, S.D. Lee, B.G. Lee, H.S. Kim, Appl. Catal. A 215 (2001) 1.
[7] C. Song, K.M. Reddy, Appl. Catal. A 176 (1999) 1.
[8] G.A. Deluga, J.R. Salge, L.D. Schmidt, X.E. Verykios, Science 303 (2004) 993.
[9] V.V. Galvita, G.L. Semin, V.D. Belyaev, T.M. Yurieva, V.A. Sobyanin, Appl. Catal. A 216 (2001) 85.
[10] Y. Tanaka, R. Kikuchi, T. Takeguchi, K. Eguchi, Appl. Catal. B 57 (2005) 211.
[11] T.A. Semelsberger, K.C. Ott, R.L. Borup, H.L. Greene, Appl. Catal. A 309 (2006) 210.
[12] Y. Tanaka, T. Utaka, R. Kikuchi, K. Sasaki, K. Eguchi, Appl. Catal. A 238 (2003) 11.
[13] Q. Fu, W. Deng, H. Saltsburg, M. Flytzani-Stephanopoulos, Appl. Catal. B 56 (2005) 57.
[14] N. Schumacher, A. Boisen, S. Dahl, A.A. Gokhale, S. Kandoi, L.C. Grabow, J.A. Dumesic, M. Mavrikakis, I. Chorkendorff, J. Catal. 229 (2005) 265.
[15] T. Tabakova, F. Boccuzzi, M. Manzol, J.W. Sobczak, V. Idakiev, D. Andreeva, Appl. Catal. B 49 (2004) 73.
[16] M.M. Schubert, A. Venugopal, M.J. Kahlich, V. Plzak, R.J. Behm, J. Catal. 222 (2004) 32.
[17] F. Mariño, C. Descorme, D. Duprez, Appl. Catal. B 54 (2004) 59.

[18] O. Pozdnyakova, D. Teschner, A. Wootsch, J. Kröhnert, B. Steinhauer, H. Sauer, L. Toth, F.C. Jentoft, A. Knop-Gericke, Z. Paál, R. Schlögl, J. Catal. 237 (2006) 1.
[19] W.B. Kim, T. Voitl, G.J. Rodriguez-Rivera, S.T. Evans, J.A. Dumesic, Angew. Chem. Int. Ed. 44 (2005) 778.
[20] W.B. Kim, T. Voitl, G.J. Rodriguez-Rivera, J.A. Dumesic, Science 305 (2004) 1280.
[21] Lambiotte and Cie, online publications (http://www.lambiotte.com/methylal.html).
[22] S. Satoh, Y. Tanigawa, US Patent 6 379 507, 2002.
[23] Y. Yuan, T. Shido, Y. Iwasawa, Chem. Commun. (2000) 1421.
[24] H. Liu, N. Bayat, E. Iglesia, Angew. Chem. Int. Ed. 42 (2003) 5072.
[25] K. Fuji, S. Nakano, E. Fujita, Synthesis (1975) 276.
[26] J. Masamoto, T. Iwaisako, M. Chohno, M. Kawamura, J. Ohtake, K. Matsuzaki, J. Appl. Polym. Sci. 50 (1993) 1299.
[27] Q. Sun, A. Auroux, J. Shen, J. Catal. 244 (2006) 1.
[28] J.-P. Shen, C. Song, Catal. Today 77 (2002) 89.
[29] B.A. Peppley, J.C. Amphlett, L.M. Kearns, R.F. Mann, Appl. Catal. A 179 (1999) 31.
[30] T. Barzetti, E. Selli, D. Moscotti, L. Forni, J. Chem. Soc. Faraday Trans. 92 (1996) 1401.
[31] J. Shen, M.J. Lochhead, K.L. Bray, Y. Chen, J.A. Dumesic, J. Phys. Chem. 99 (1995) 2384.
[32] A. Chambers, T. Nemes, N.M. Rodriguez, R.T.K. Baker, J. Phys. Chem. B 102 (1998) 2251.
[33] A. Dandekar, R.T.K. Baker, M.A. Vannice, J. Catal. 183 (1999) 131.
[34] G.L. Bezemer, P.B. Radstake, V. Koot, A.J. van Dillen, J.W. Geus, K.P. de Jong, J. Catal. 237 (2006) 291.
[35] X. Dong, H.-B. Zhang , G.-D. Lin, Y.-Z. Yuan, K.R. Tsai, Catal. Lett. 85 (2003) 237.
[36] T.G. Ros, A.J. van Dillen, J.W. Geus, D.C. Koningsberger, Chem. Eur. J. 8 (2002) 1151.
[37] M.L. Toebes, J.M.P. van Heeswijk, J.H. Bitter, A.J. van Dillen, K.P. de Jong, Carbon 42 (2004) 307.
[38] C. Hong, Z. Zhang, J. Cao, D. Qiu, Y. Li, Y. Fu, CN Patent 1 356 169, 2003.
[39] C. Hong, Z. Zhang, J. Cao, D. Qiu, Y. Li, Y. Fu, CN Patent 1 356 166, 2004.
[40] J. Shen, Q. Sun, H. Zhang, CN Patent 1 562 468, 2006.
[41] G.C. Chinchen, C.M. Hay, H.D. Vanderwell, K.C. Waugh, J. Catal. 103 (1987) 79.
[42] M. Li, J. Shen, J. Catal. 205 (2002) 248.
[43] T. Takeguchi, K.-I. Yanagisawa, T. Inui, M. Inoue, Appl. Catal. A 192 (2000) 201.
[44] X.-M. Liu, G.Q. Lu, Z.-F. Yan, J. Beltramini, Ind. Eng. Chem. Res. 42 (2003) 6518.
[45] I.E. Wachs, R.J. Madix, J. Catal. 53 (1978) 208.
[46] I.A. Fisher, A.T. Bell, J. Catal. 184 (1999) 357.
[47] C.J. Jiang, D.L. Trimm, M.S. Wainwright, N.W. Cant, Appl. Catal. A 97 (1993) 145.
[48] G.C. Chinchen, M.S. Spencer, K.C. Waugh, D.A. Whan, J. Chem. Soc. Faraday Trans. I 83 (1987) 2193.